UMR
UNIVERSITY OF MISSOURI-ROLLA

CENTER FOR INFRASTRUCTURE ENGINEERING STUDIES

The Effect of Fatigue on Understrength Shear-Critical Reinforced Concrete Beams Reinforced with External CFRP Stirrups

By

Andrew Budek

Jedediah Taylor

Philip Nash

University Transportation Center Program at the University of Missouri-Rolla

Disclaimer

The contents of this report reflect the views of the author(s), who are responsible for the facts and the accuracy of information presented herein. This document is disseminated under the sponsorship of the Department of Transportation, University Transportation Centers Program and the Center for Infrastructure Engineering Studies UTC program at the University of Missouri - Rolla, in the interest of information exchange. The U.S. Government and Center for Infrastructure Engineering Studies assumes no liability for the contents or use thereof.

Technical Report Documentation Page

1. Report No.	2. Government Accession No.	3. Recipient's Catalog No.
UTC R144		

4. Title and Subtitle	5. Report Date
The Effect of Fatigue on Understrength Shear-Critical Reinforced Concrete Beams Reinforced with External CFRP Stirrups	January 2007
	6. Performing Organization Code

7. Author/s	8. Performing Organization Report No.
Andrew Budek, Jedediah Taylor, Philip Nash	00001406/0008404

9. Performing Organization Name and Address	10. Work Unit No. (TRAIS)
Center for Infrastructure Engineering Studies/UTC program University of Missouri - Rolla 223 Engineering Research Lab Rolla, MO 65409	11. Contract or Grant No. DTRS98-G-0021

12. Sponsoring Organization Name and Address	13. Type of Report and Period Covered
U.S. Department of Transportation Research and Special Programs Administration 400 7th Street, SW Washington, DC 20590-0001	Final
	14. Sponsoring Agency Code

15. Supplementary Notes

16. Abstract

This is a technical report detailing the testing of six understrength reinforced concrete beams subjected to fatigue loading. Three beams were tested as-built, and three were reinforced with external carbon fiber stirrups. Tests to failure of as-built/retrofitted beam pairs were conducted statically, and after 100,000 and 1,000,000 cycles respectively. The beams subjected to fatigue loading were first loaded quasi-statically to first cracking. The load amplitude for fatigue was set to give a peak load at 75% of that for first cracking. The as-built beams failed through rupture of the internal steel shear reinforcement. The CFRP beams failed through rupture of the concrete under the CFRP-concrete interface. The load distribution mechanism in the fatigue loaded CFRP-reinforced beams was different from the statically loaded example in that the strains in the CFRP were substantially higher through the post-fatigue loading regime. This suggests that the crack surfaces were 'worked', or polished by fatigue loading, degrading the concrete shear-resisting mechanism. The CFRP-reinforced beams also displayed different crack patterns from the unreinforced examples, in that a small number of wide shear cracks formed, inclined at 45◦. Cracking in the as-built specimens was more widely spread, and the cracks were narrower. The force-displacement response of CFRP-reinforced beams was found to be bilinear in all cases, as was the response of the as-built beam subjected to 1,000,000 cycles. The as-built beams subjected to no cyclic loading, and 100,000 cycles, had a linear force-displacement response. An equation is presented which predicts ultimate shear strength of the CFRP-reinforced beams within an LRFD framework.

17. Key Words	18. Distribution Statement
Understrength, Reinforced concrete, Beams, Fatigue loading, Carbon fiber, Test to failure, Retrofitting, Shear reinforcement, CFRP, Post-fatigue loading, Cracks, Force-displacement, Ultimate shear strength, LRFD	No restrictions. This document is available to the public through the National Technical Information Service, Springfield, Virginia 22161.

19. Security Classification (of this report)	20. Security Classification (of this page)	21. No. Of Pages	22. Price
unclassified	unclassified	20	

Form DOT F 1700.7 (8-72)

The Effect of Fatigue on Understrength Shear-Critical Reinforced Concrete Beams Reinforced with External CFRP Stirrups

Andrew Budek, Department of Civil and Environmental Engineering, Texas Tech University, P.O. Box 41023, Lubbock, TX 79409-1023

Jedediah Taylor, Department of Civil and Environmental Engineering, Texas Tech University

Philip Nash, Department of Civil and Environmental Engineering, Texas Tech University

ACKNOWLEDGEMENTS

The PI would like to thank the University of Missouri, the U.S. Department of Transportation, the College of Engineering at Texas Tech University, Sika Corporation, and his colleagues, Mr. Jedediah Taylor and Mr. Philip Nash.

Most of all, the PI would like to thank his wife, Barbara.

ABSTRACT

This is a technical report detailing the testing of six understrength reinforced concrete beams subjected to fatigue loading. Three beams were tested as-built, and three were reinforced with external carbon fiber stirrups. Tests to failure of as-built/retrofitted beam pairs were conducted statically, and after 100,000 and 1,000,000 cycles respectively. The beams subjected to fatigue loading were first loaded quasi-statically to first cracking. The load amplitude for fatigue was set to give a peak load at 75% of that for first cracking. The as-built beams failed through rupture of the internal steel shear reinforcement. The CFRP beams failed through rupture of the concrete under the CFRP-concrete interface. The load distribution mechanism in the fatigue loaded CFRP-reinforced beams was different from the statically loaded example in that the strains in the CFRP were substantially higher through the post-fatigue loading regime. This suggests that the crack surfaces were 'worked', or polished by fatigue loading, degrading the concrete shear-resisting mechanism. The CFRP-reinforced beams also displayed different crack patterns from the unreinforced examples, in that a small number of wide shear cracks formed, inclined at 45◦. Cracking in the as-built specimens was more widely spread, and the cracks were narrower. The force-displacement response of CFRP-reinforced beams was found to be bilinear in all cases, as was the response of the as-built beam subjected to 1,000,000 cycles. The as-built beams subjected to no cyclic loading, and 100,000 cycles, had a linear force-displacement response. An equation is presented which predicts ultimate shear strength of the CFRP-reinforced beams within an LRFD framework.

SPECIMEN CONSTRUCTION AND TEST SETUP

The specimens were beams of 5” width and 10” overall depth. They were a total of 54” long; the test length was 30” long.

Steel reinforcement consisted of two #7 Gr. 60 bars placed at a depth d = 8.5”, and #3 Gr. 60 stirrups placed at 6” on center. This spacing was chosen to ensure that the beams would be under-reinforced, and allow failure within the capacity of the testing equipment, and still have a stirrup crossing the presumptive plane of shear cracking.

The CFRP-reinforced beams had external stirrups made from one layer of Sikawrap™ carbon fiber fabric, ½” wide. They were attached with Sika Hex300D™ two-part epoxy.

The test rig consisted of a steel reaction beam with roller supports at 30”, placed on a 55-kip MTS Universal Testing Machine. The geometry of the reaction beam and rollers was such that the load was applied at the specimens’ 1/3 points. The load was applied by the UTM’s ram through a masonry leveling pad and a thick steel plate. The beam lay directly on the rollers. This allowed local crushing but was deemed more acceptable than a bearing plate, which may have provided confinement and altered shear response.

Strain gauges were placed on CFRP strips and steel stirrups in the high-shear region. The strain gauges were placed in a position corresponding to the mid-depth of the beam. Load-point displacement and force were measured.

Load was applied in 1-kip increments to first cracking, in 2-kip increments until within 20% of the estimated ultimate load, and then in 1-kip increments to failure.

Specimen and loading geometry are shown in Fig. 1. In the description and discussion of results, the part of the beam between the left-hand roller support (in Fig. 1) and the load application point is referred to as the high-shear region. The part of the beam to the right of the load point is called the low-shear region. The test setup is shown in Fig. 2.

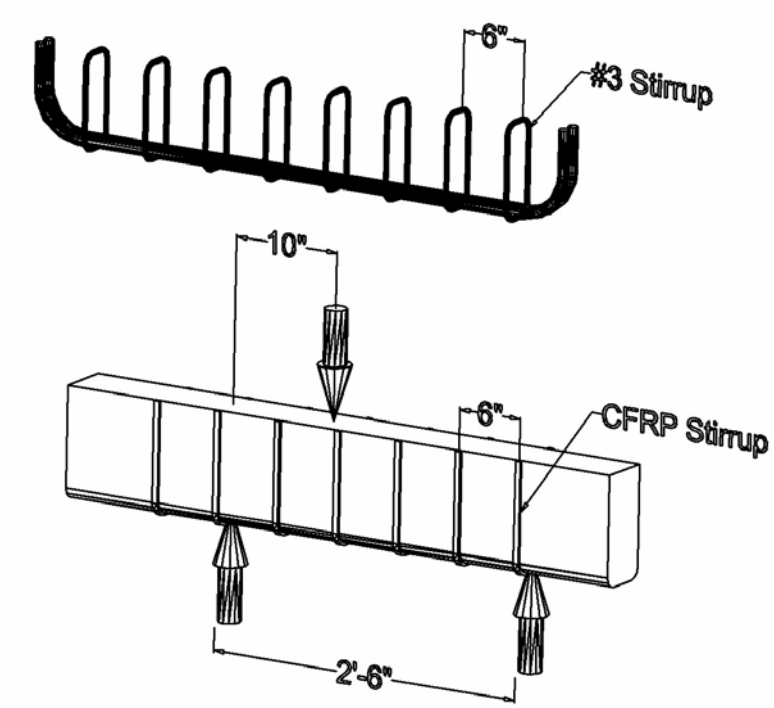

Fig. 1 – Beam, reinforcement, and loading geometry

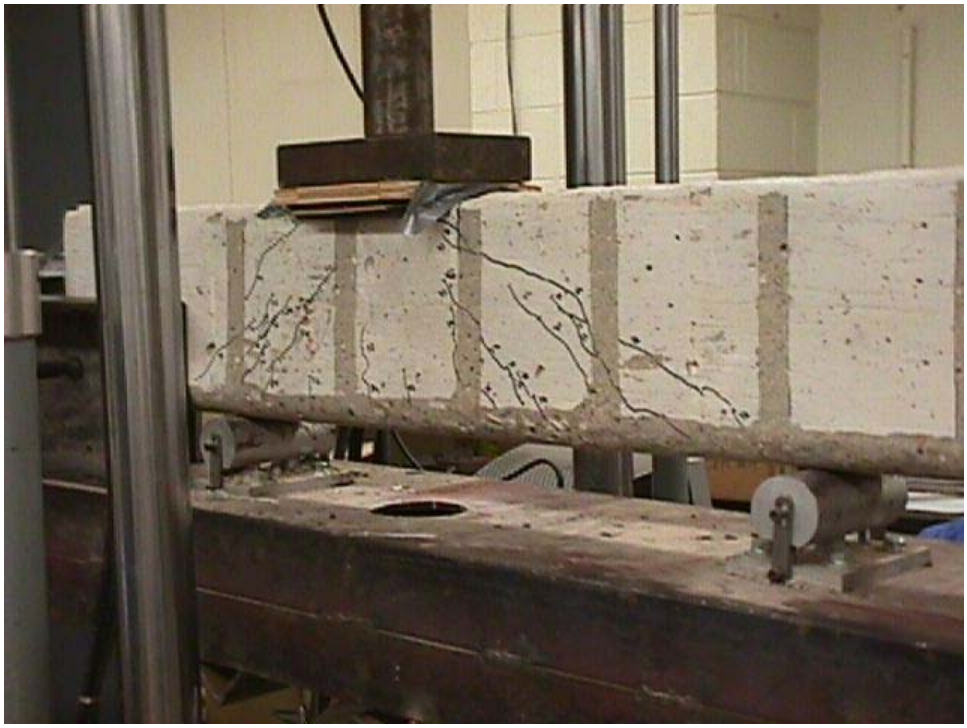

Fig. 2 – Test setup

The test matrix consisted of six beams (Table 1). Three were as-built (no CFRP), and three had CFRP reinforcement. Two of each as-built/CRFP-reinforced 'pair' were tested statically. The second pair were loaded to first cracking, then cycled at 75% of the first

cracking load for 100,000 cycles, and finally loaded to failure. The third pair were loaded to first cracking, cycled at 75% of the cracking load for 1,000,000 cycles, and then loaded quasi-statically to failure.

Table 1 – Test matrix

Beam	Description	Static	100,000 cycles	1,000,000 cycles
1	As-Built	X		
2	As-Built		X	
3	CFRP-reinforced	X		
4	CFRP-reinforced		X	
5	As-Built			X
6	CFRP-reinforced			X

Day-of-test material properties are shown in Table 2. Due to an equipment casualty, actual values for the strength and elastic modulus of the steel stirrups (f_y) and the CFRP straps (f_{cf}) could not be taken; assumed values taken from literature are shown.

Table 2 – Day-of-Test Material Properties

Beam	f_c'	f_y	E_{steel}	f_{cf}	E_{cf}
1	2.55 ksi	60 ksi	29,000 ksi		
2	2.75 ksi	60 ksi	29,000 ksi		
3	3.24 ksi	60 ksi	29,000 ksi	150 ksi	25,000 ksi
4	2.99 ksi	60 ksi	29,000 ksi	150 ksi	25,000 ksi
5	3.53 ksi	60 ksi	29,000 ksi		
6	2.99 ksi	60 ksi	29,000 ksi	150 ksi	25,000 ksi

RESULTS

Beam 1, an as-built specimen, was tested statically to failure. Its force-displacement response is shown in Fig. 3. Cracking was first observed at a shear force of 9.38 kips. Though there is a slight discontinuity in the force-displacement response close to this value, it was ascertained to be an artifact of the data-collection method. Cracking continued through the loading program until failure. The cracks observed in the high-shear region (i.e., the shorter span between the point of load application and the closer support) were inclined at 45◦. Cracking was first observed in the vicinity of the neutral axis, and as loading progressed spread symmetrically toward the top and bottom of the beam along the general 45◦ inclination of the original cracks. Several sets of parallel cracks were recorded. Crack widths were quite narrow as the shear strain was spread over a relatively wide area. As the beam progressed toward failure, crack widths in the high-

shear region increased to a maximum of 0.01 in. On the lower-shear side of the beam, cracking was seen to be at a shallower inclination (about 30◦), and the cracks were wider (maximum width of about 0.02 in). A typical crack pattern for an as-built beam is shown in Fig. 4.

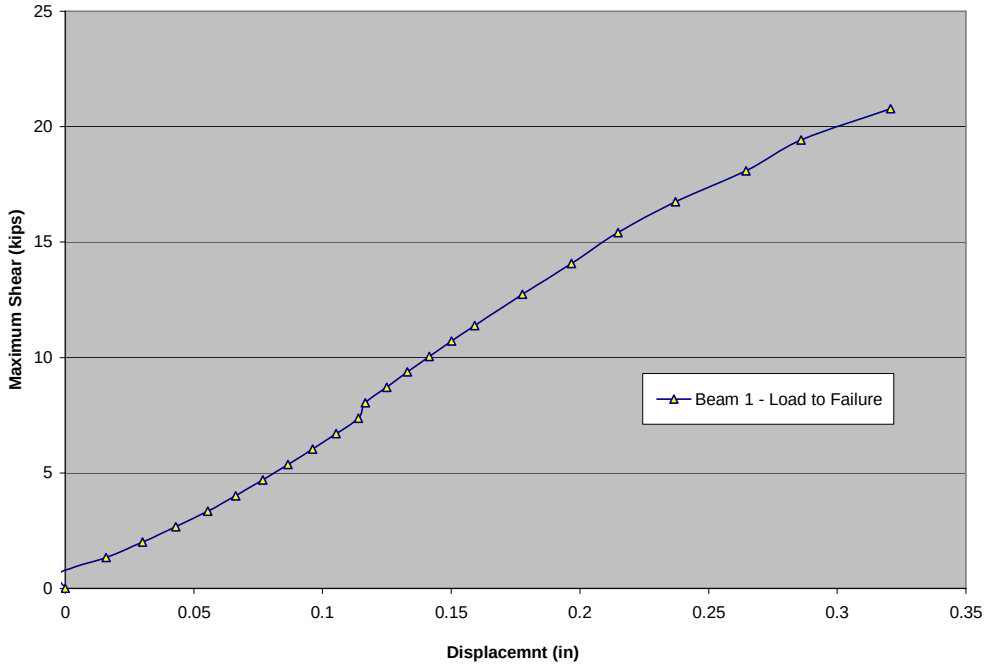

Fig. 3 – Beam 1 force-displacement (as-built, quasi-static loading; failure at V=22.11 k, before displacement measurement could be taken)

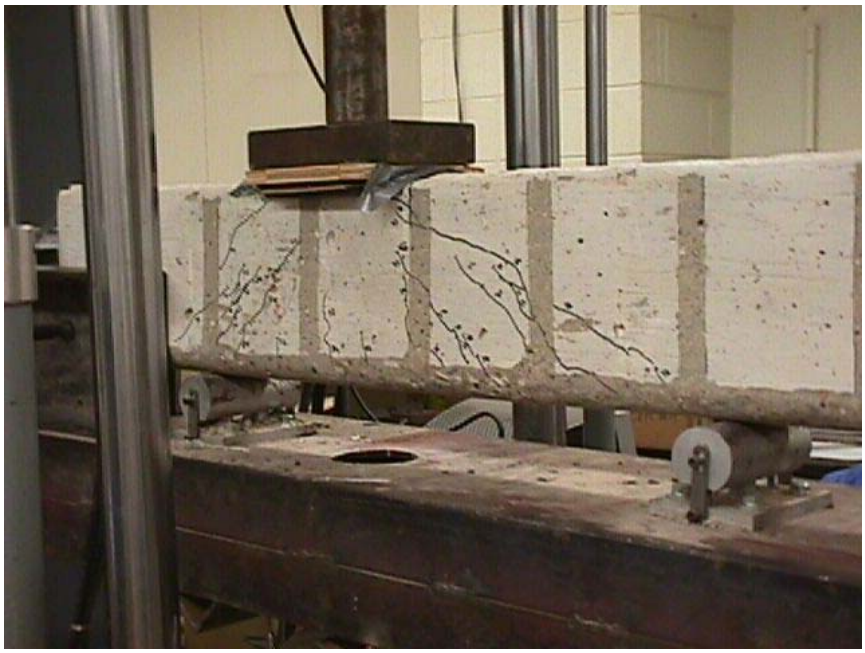

Fig. 4 – Crack patterns in Beam 1

The strains in the steel stirrups in the high-shear region of Beam 1 are shown in Fig. 5. This data clearly shows that a large amount of the applied shear force was transferred to the stirrups at a point very close to the maximum capacity of the beam. This indicates that the concrete-shear-resisting mechanism was performing competently through nearly the entire loading regime, and that the crack widths recorded were commensurate with this competent concrete performance

Even though the shear span was very low (M/VD ≈ 1.17) this beam did not show deep-beam behavior. The crack patterns and overall response were consistent with the performance of a beam outside the D-region. Indeed, none of the beams tested showed deep-beam behavior.

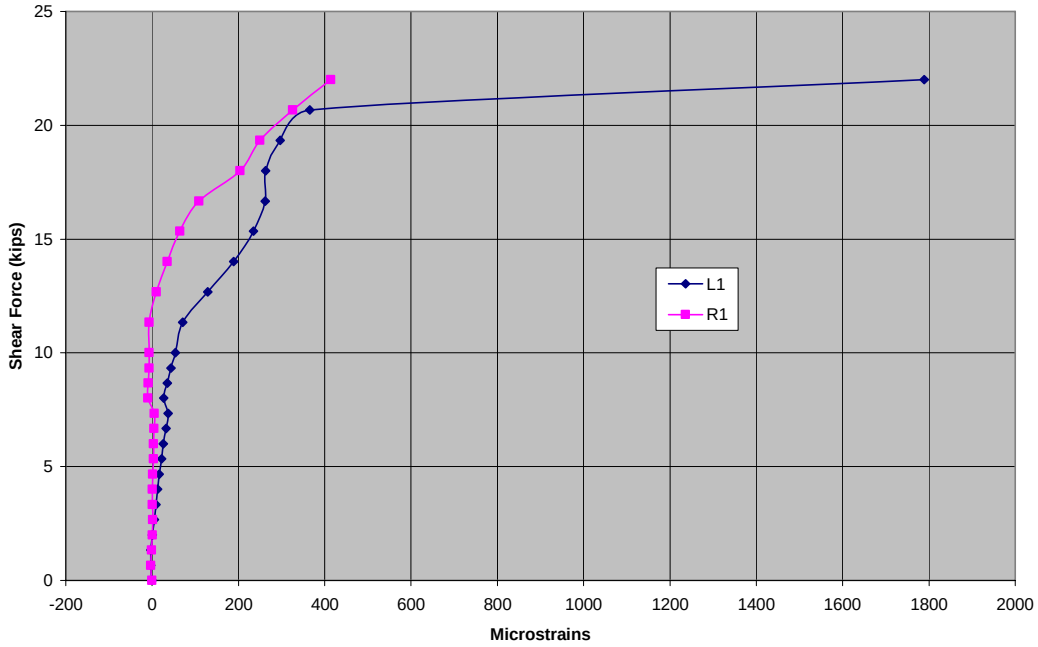

Fig. 5 – Beam 1 steel stirrup strains in the high shear region

In Fig. 6, the force-displacement response of Beam 2 is shown. Beam 2 was as-built, cycled 100,000 times at a load level 75% of first cracking. (The data from the initial loading was lost.) Fig. 6 reflects the response of the beam in its final quasi-static loading to failure. The performance of this beam was similar to Beam 1; the response was nearly linear to failure, and there was no change in stiffness associated with the onset of cracking. Crack patterns and widths were similar to those seen in Beam 1. The large initial displacement was an artifact caused by seating of the specimen and loading pad.

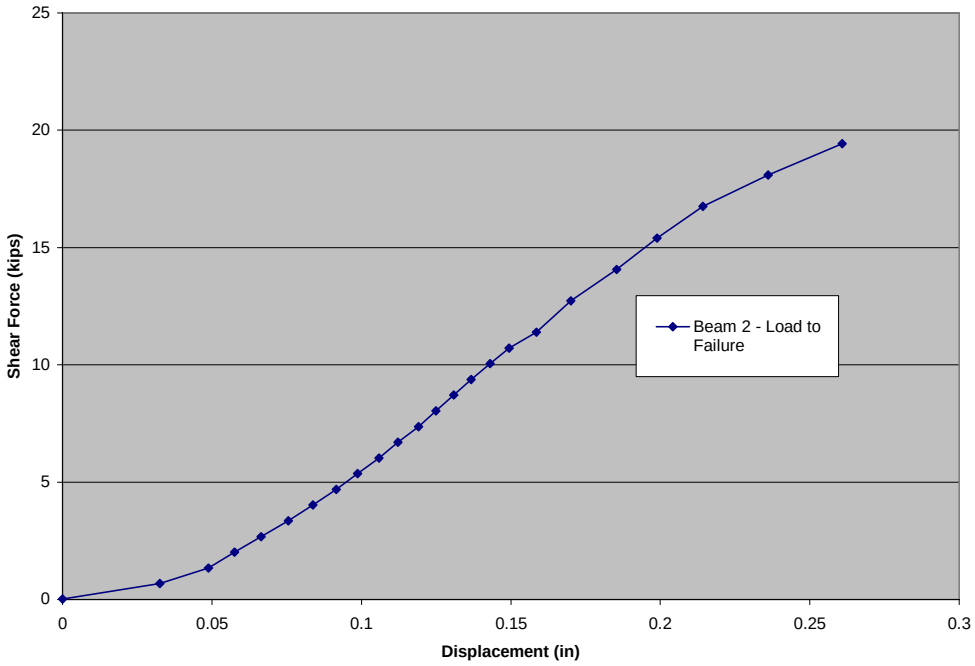

Fig. 6 – Beam 2 force-displacement (as-built, quasi-static loading after 100,000 fatigue cycles; failure occurred at V = 20.77 k, before displacement reading could be taken)

Steel stirrup strains in the high-shear region of Beam 2 are shown in Fig. 7. As in the case of Beam 1, strains were relatively low until close to failure, at which point they started to increase. Data from the last load step is missing. However, the trend of existing data is consistent with the response of Beam 1 (i.e., competent performance of the concrete shear mechanism until close to failure).

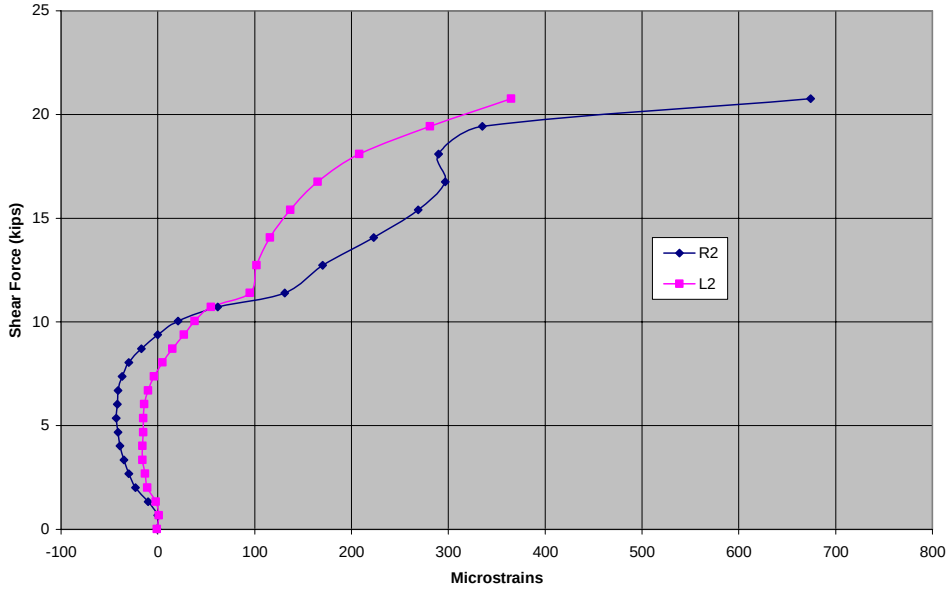

Fig. 7 – Beam 2 steel stirrup strains (as-built; quasi-static loading to failure after loading at 75% of first cracking)

The force-displacement response of Beam 3 is shown in Fig. 8. Beam 3 was reinforced with external carbon-fiber straps along with internal stirrups, and was tested statically to failure. The maximum shear force recorded was about 50% higher than that seen in the as-built Beams 1 and 2. (The large displacement at initial loading was an artifact caused by seating of the beam and loading pad.) The response of Beam 3 was somewhat different from the as-built specimens. The initial stiffness was greater, which indicates that most of the displacement recorded was shear displacement.

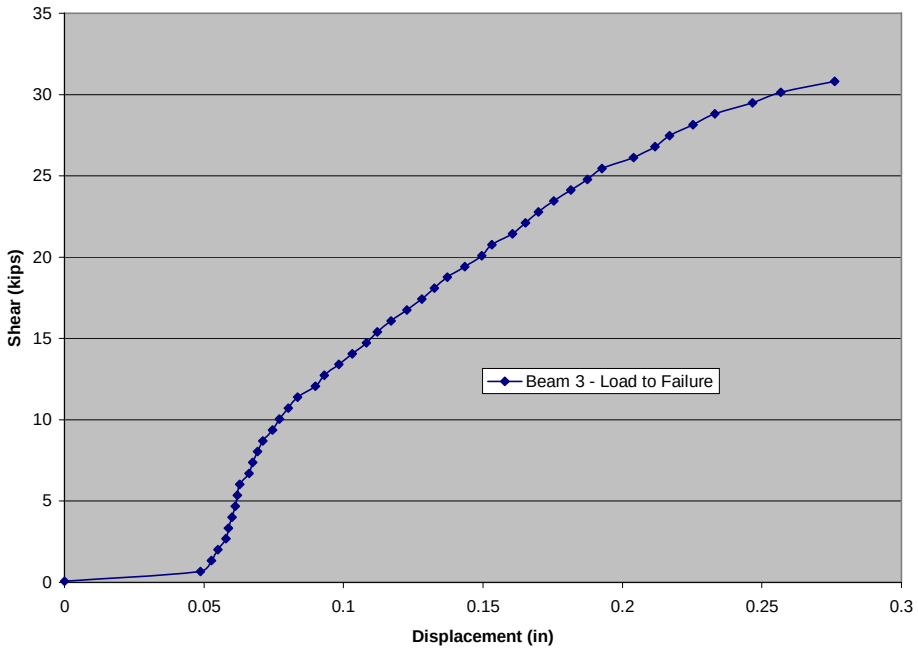

Fig. 8 - Beam 3 force-displacement (CFRP – quasi-static loading)

First cracking was seen in the high-shear region at a shear force of 9.38 kips, which is consistent with that observed in the as-built Beams 1 and 2. There is a reduction in structural stiffness which is consistent with the load level at which cracking began. The crack patterns which developed in the high- and low-shear regions were fundamentally different from those observed in the as-built specimens. In Beam 3, there was 'one big crack' with extensions; additional small cracks did develop, but the bulk of crack growth and widening was associated with the original one. Initially this crack stopped at a CFRP strap; as loading progressed it turned 'north' (toward the top of the beam) for about ½", and then resumed its original 45◦ inclination to pass under the strap.

The first crack in the low-shear region was seen at a level of shear force similar to that which formed the first high-shear-side crack. This first crack passed under a carbon fiber strap. As in the case of the as-built specimens, low-shear region cracking had a shallower inclination. The high-shear region crack pattern for Beam 3 at a shear of 20.77 kips is shown in Fig. 9 (this is a typical crack pattern for the CFRP-reinforced beams tested). The low-shear region crack pattern at the same load level (corresponding to V=10.39 kips in that region) is shown in Fig. 10.

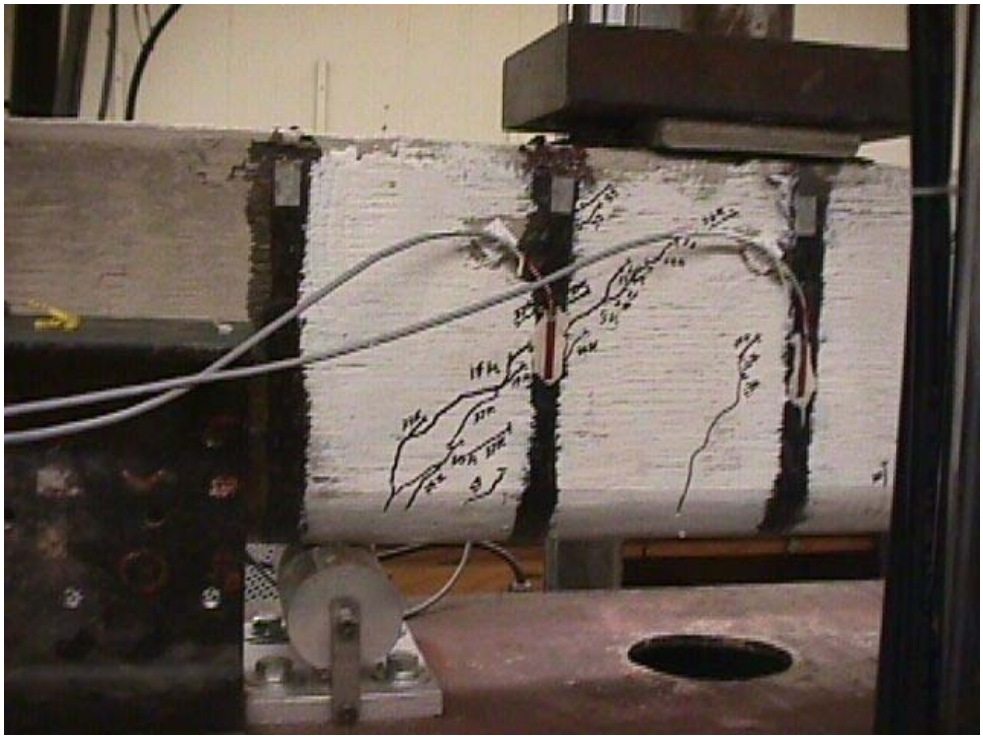

Fig. 9 – High-shear region crack pattern for Beam 3 (CF – static) at V=21 kips

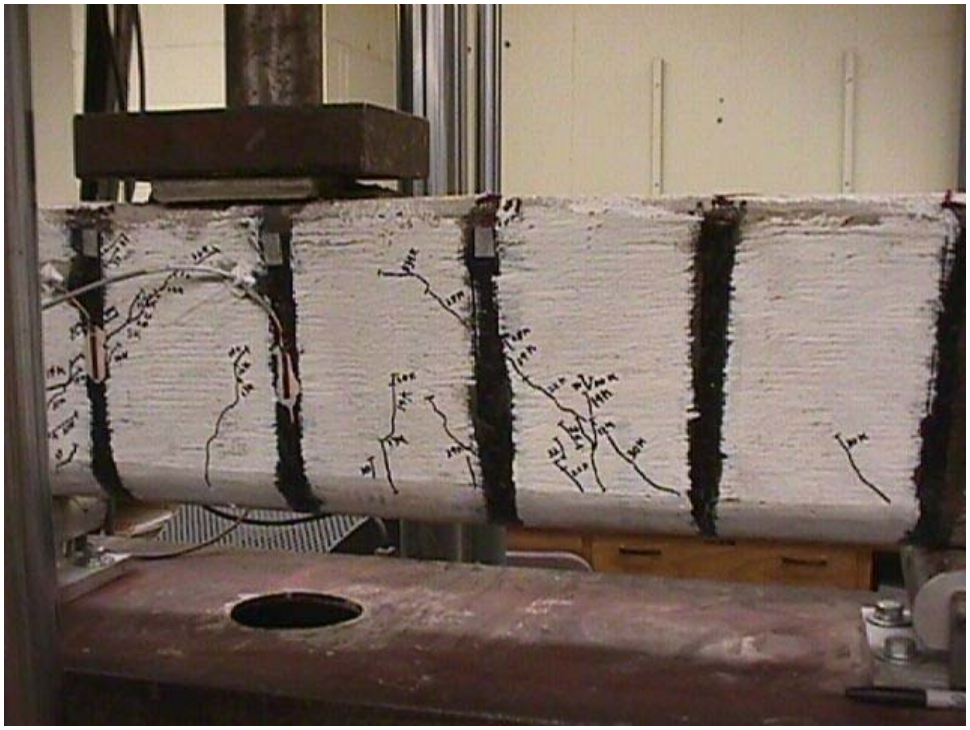

Fig. 10 – Low-shear region crack pattern for Beam 3

Recorded steel stirrup strains in the high-shear region of Beam 3 are shown in Fig. 11 (only one strain gauge in this region survived). This clearly shows a progressive mobilization of the steel reinforcement in resisting shear. This can be associated with the formation of a limited number of wide cracks, which was apparently driven by the presence of the CFRP reinforcement. This degraded the concrete shear-resisting mechanism, and forced the more active participation of the steel, when compared to the beams that did not have CFRP reinforcement.

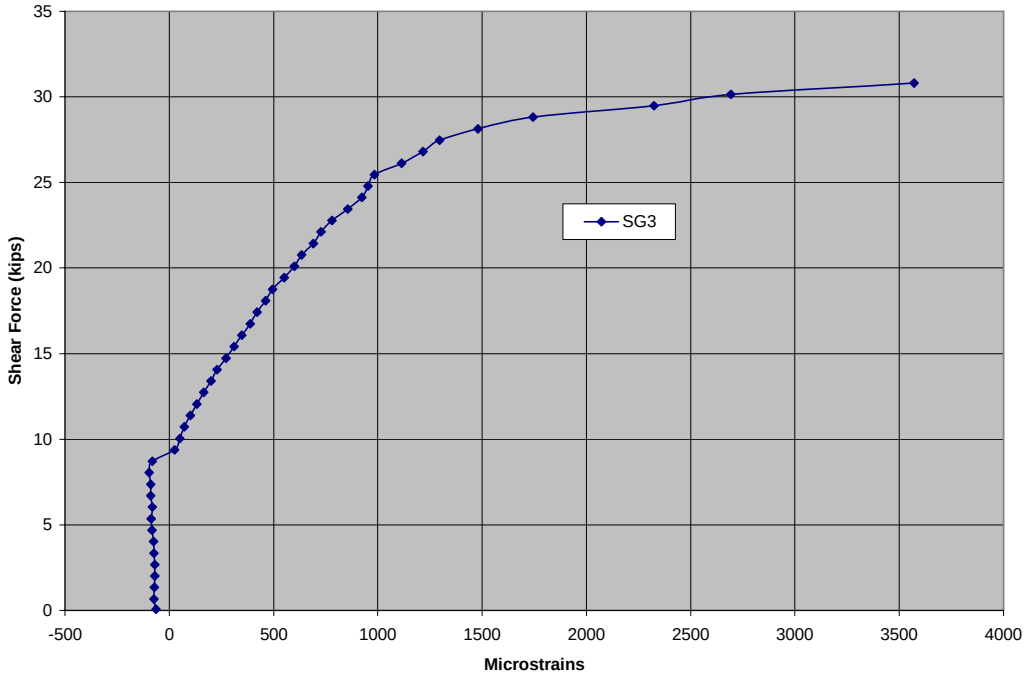

Fig. 11 – Steel stirrup strains in high-shear region of Beam 3 (CFRP – quasi-static loading)

The strains in the CFRP reinforcement in the high-shear region of Beam 3 are shown in Fig. 12. These strains are relatively low; they certainly do not show that the bulk of shear force is being borne by the CFRP. These results point to an active participation by all three shear-resisting mechanisms (concrete, steel, CFRP).

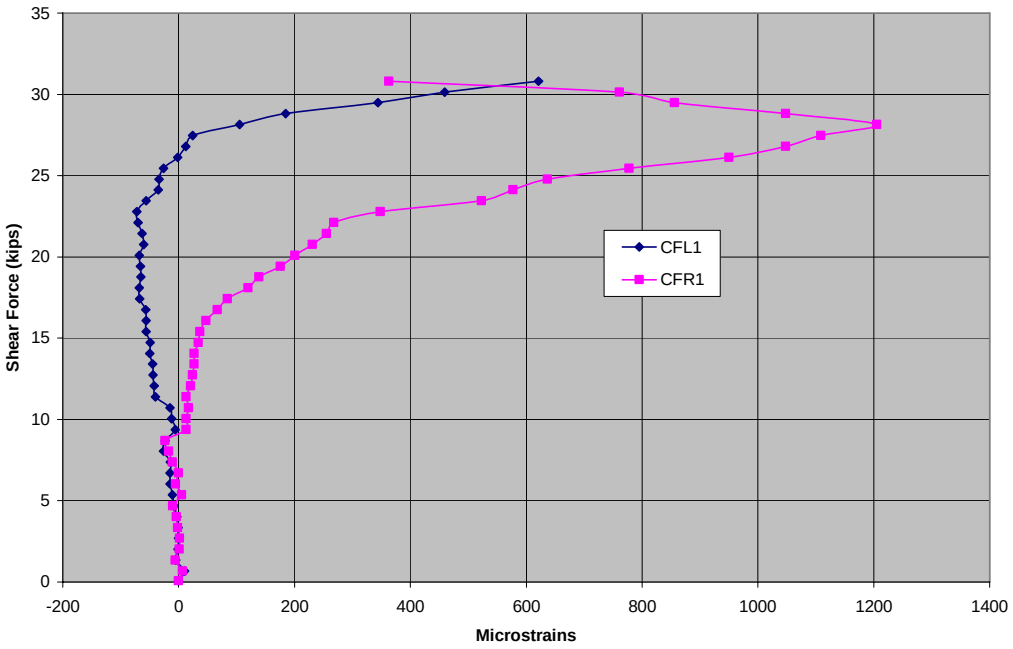

Fig. 12 – Beam 3 carbon fiber strap strains in high-shear region (CFRP – quasi-static loading)

Failure of Beam 3 came through rupture of the concrete under the CFRP reinforcement in the high-shear region, followed immediately by rupture of the associated steel stirrup. The concrete under the CFRP failed over about 75% of the beam depth.

Fig. 13 – CFRP debonding in failure of Beam 3

The force-displacement response of Beam 4 is shown in Fig. 14. Beam 4, externally reinforced with CFRP, was initially loaded to first cracking, and then cycled 100,000 times from 1 kip to a load equivalent to 75% of the first cracking load. It was then loaded quasi-statically to failure. In the final loading there was a possible slight increase in stiffness at a load in the vicinity of the first cracking load, which may represent the carbon fiber being mobilized. At a shear load around 23 kips there was a definite reduction in stiffness; second slope stiffness is about half of the original value. This bilinear response continued until failure. The failure mode was fracture of the concrete for about 75% of the beam depth under the carbon-fiber strap in the high-shear region, followed by immediate rupture of the associated steel stirrup, as in Beam 3.

Cracking in Beam 4 during the final loading sequence (after fatigue loading) took a similar pattern as seen in beam 3; however, the cracks were substantially wider. The width prior to failure was measured at 0.02 in. This is about twice the width of the widest cracks in Beam 3.

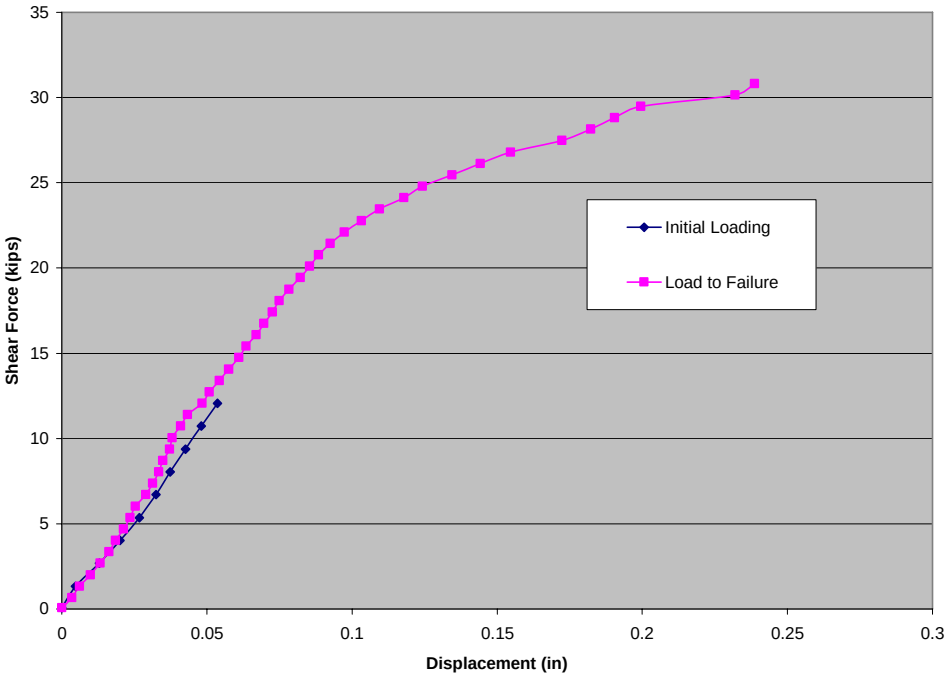

Fig. 14 – Beam 4 force-displacement (CFRP, initial quasi-static loading and quasi-static loading after 100k cycles)

The strain gauges on the steel reinforcement in the high-shear region unfortunately did not survive casting; however, the strain gauges from the carbon fiber straps in the high-shear region (Fig. 15) give some interesting information. Very low strains are seen in the initial loading to first cracking. After cycling, however, the strains are much higher than those seen at comparable loads in Beam 3. This corresponds to greater crack widths, and indicates that the CFRP was much more highly mobilized after cycling of the cracked specimen. This suggests that cycling degraded the concrete shear-resisting mechanism,

perhaps by ‘polishing’ the crack surfaces and reducing the effectiveness of aggregate interlock.

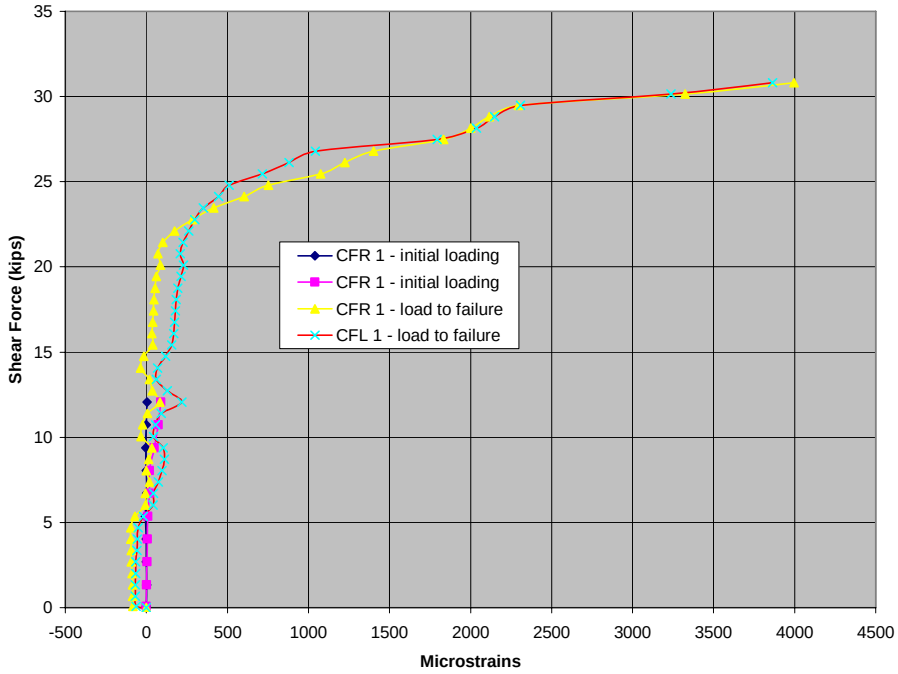

Fig. 15 – Beam 4 carbon fiber strap strains in the high-shear region through initial quasi-static loading to cracking, and quasi-static loading after 100,000 fatigue cycles

Beam 5 was an as-built beam. It was first loaded quasi-statically to first cracking, and then cycled 1,000,000 times at a load 75% of that which caused cracking. Its force-displacement response is shown in Fig. 16. Notable is the reduction in stiffness after cycling. The final loading of Beam 5 also produced a pronounced bilinear response.

Cracking in both the high- and low-shear regions of Beam 5 followed the pattern seen in Beams 1 and 2. A network of shear cracks inclined at 45◦ formed in the high-shear region, and a more shallowly inclined network formed in the low-shear region. Crack widths in the high-shear region reached a maximum of 0.01 in, while the cracks in the low-shear region were wider, at 0.025 in.

Failure of Beam 5 at a shear force of 31 kips came through rupture of the steel shear reinforcement in the high-shear region.

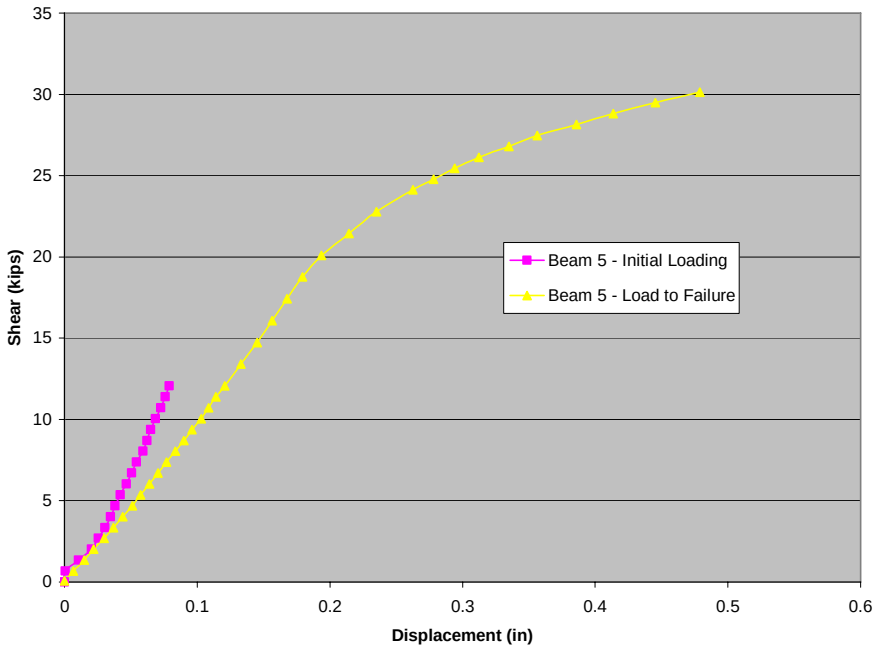

Fig. 16 – Beam 5 force-displacement (as-built, initial quasi-static loading and quasi-static loading after 1M cycles; failure at V=31 k, before displacement could be measured)

Steel stirrup strains in Beam 5 are shown in Fig. 17. While the final readings at V = 31 kips could not be taken, the results that are available show a progressive mobilization of the shear reinforcement.

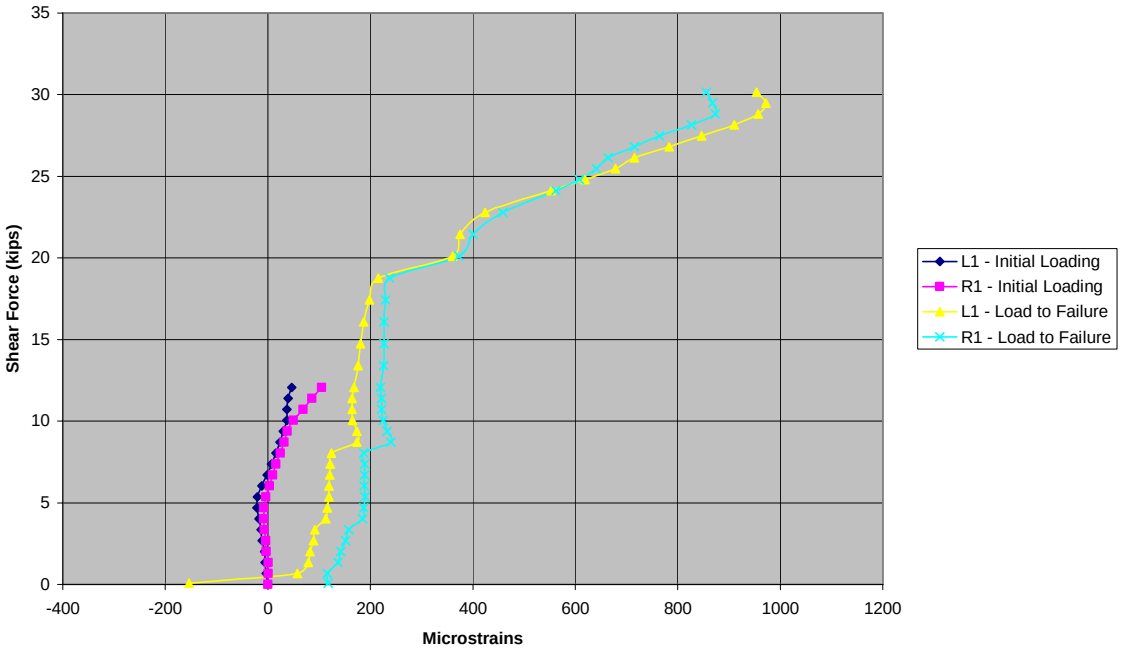

Fig. 17 – Beam 5 steel stirrup strains in the high-shear region for initial quasi-static loading, and quasi-static loading after 1,000,000 fatigue cycles.

The force-displacement response of Beam 6 is shown in Fig. 18. Beam 6 had external CFRP reinforcement. It was loaded quasi-statically to first cracking, and then cycled from 1 kip to 75% of the initial cracking load for 1,000,000 cycles. It was then loaded quasi-statically to failure. The response is clearly bilinear, and there is no discernable difference in stiffness between initial and final quasi-static loading. (The discontinuity at 10 kips in the final loading sequence is a measurement artifact.) The second-slope stiffness is much lower than that recorded in the as-built Beam 5. Since the reinforcement can be assumed to carry a large part of the shear in this part of the loading sequence, this can be assumed to indicate the lower stiffness of the CFRP when compared to steel.

Cracking was similar to than seen in Beams 3 and 4. Wide single cracks, with smaller late-forming auxiliary cracks, were seen in the high- and low-shear regions.

Failure at V = 29 kips was also similar to Beams 3 and 4. The concrete under the carbon fiber straps in the high-shear regions ruptured through about 75% of the beam depth. This was immediately followed by failure of the steel shear reinforcement.

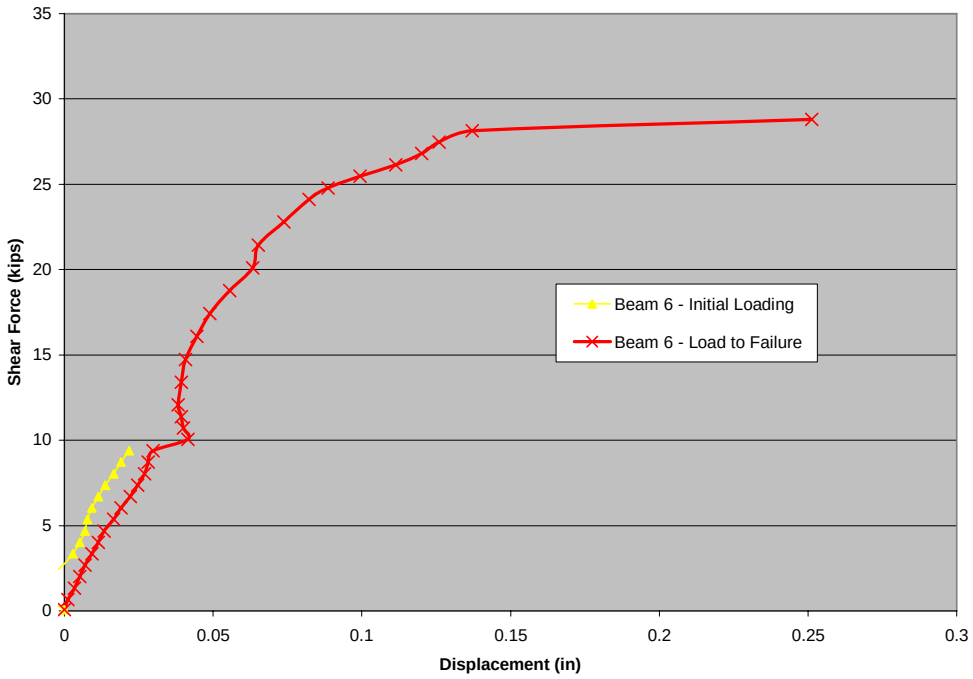

Fig. 18 - Beam 6 force-displacement (CFRP, initial static loading and static loading after 1,000,000 cycles)

The steel stirrup strains in the high-shear region of Beam 6 are shown in Fig. 19. Only one gauge survived casting. The initial loading, to cracking, was clearly borne by the concrete, with minimal steel reinforcement contribution. The final loading was also largely borne by the concrete until late in the loading process, when the steel strains began to increase quickly. The strains at the final loading step could not be taken, but it may be assumed that the trend of rapid increase continued.

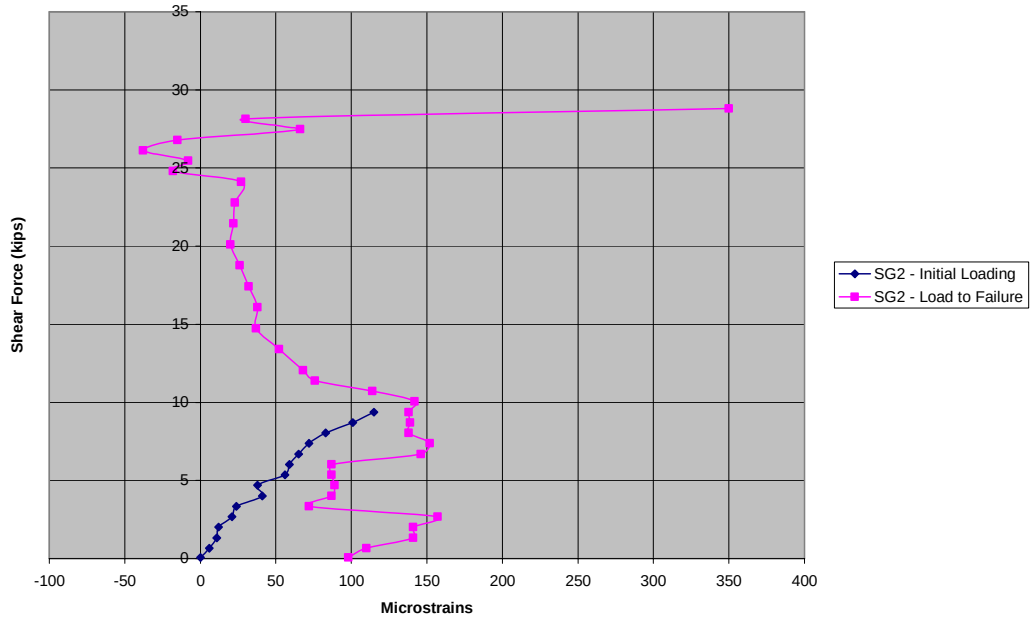

Fig. 19 – Beam 6 stirrup strains in high-shear region, initial quasi-static loading to cracking, and final quasi-static loading to cracking after 1,000,000 fatigue cycles

Strains in the carbon fiber straps in the high-shear region are shown in Fig. 20. The strains are low during initial loading, as would be expected. In the final loading, the strains increased rapidly after the load corresponding to first cracking was reached. Very high strains were developed just before failure, indicating substantial mobilization of the CFRP reinforcement.

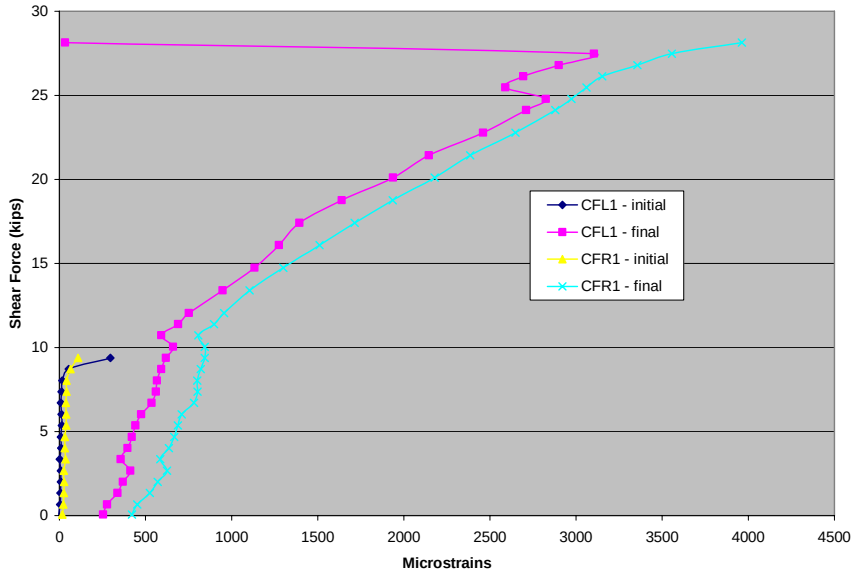

Fig. 20 - Beam 6 carbon fiber strap strains in the high-shear region through initial quasi-static loading to cracking, and quasi-static loading after 1,000,000 fatigue cycles

DISCUSSION

The results of this series of tests show some interesting points.

First, there is a definite difference in the mobilization of the carbon fiber reinforcement between the non-fatigued and fatigue tested specimens. In the non-fatigued specimen, the concrete, steel, and carbon fiber seemed to work together to carry the shear forces, until quite late in the loading processes. At this point the carbon fiber and steel strains started a rapid increase. This tendency was also seen in all of the as-built specimens (both non-fatigue and fatigue loading).

One possible explanation for this may be found in the way cracking developed. In the as-built specimens, a 'network' of cracks developed as loading progressed. These cracks were relatively narrow. This allowed for more effective aggregate interlock than can occur in a wider crack. In Beam 3, the CFRP-reinforced non-fatigue specimen, the cracks were both fewer and wider (as they were in the CRFP-reinforced fatigue specimens, Beams 4 and 6). The peak CFRP strains in Beam 3 were indicated that the straps were mobilized, but not to the degree seen in Beams 4 and 6.

This implies that in Beam 3, the load was more evenly shared between the constituents (concrete, steel, and CFRP). While the cracks were wider, the surfaces were 'fresh', and aggregate interlock was effective. The fatigue-tested specimens saw a threefold increase in strain, suggesting that the crack surfaces were worked or 'polished' by cyclic loading, degrading the effectiveness of aggregate interlock in resisting shear. This placed a proportionally larger load on the CFRP reinforcement.

The other main point observed relates to beam stiffness. The CFRP reinforced beams all showed a bilinear response after cracking, as the CFRP was mobilized in bridging the relatively wide shear cracks. The non-fatigued and 100,000 cycle as-built specimens showed a linear response to failure; however, the specimen which was subjected to 1,000,000 cycles did show a reduction in stiffness and a bilinear response. This may show a relationship between crack width and the number of cycles needed to work the surfaces to the point to which aggregate interlock is degraded, but this is only a suggestion, and needs more investigation.

A modification of the ACI beam shear analysis can be used to reasonably predict beam performance.

The ACI equation consists of two terms:

$$V_c = 2\sqrt{f_c'}b_w d \tag{1}$$

$$V_s = \frac{f_{yh}A_h d}{s} \tag{2}$$

in which f_c' is the compressive strength of the concrete, b_w is the beam width, d is the depth to the tension reinforcement, f_{yh} is the yield strength of the stirrups, A_h is the total vertical steel area (i.e., bar area times number of legs of the stirrup), and s is the stirrup spacing. These terms are added to give the nominal shear strength, and combined with the shear strength reduction factor φ=0.75 to give the LRFD equation relating demand and capacity:

$$V_u \le \phi V_n = \phi\left(V_c + V_s\right) \tag{3}$$

Since failure of the CFRP-reinforced beams was precipitated by rupture of the concrete under the strap for 75% of the beam height on each side of the beam, it is suggested that an additional capacity term taking this into account be added to Eqn. 3.

The geometry of the failure is shown in Fig. 21. The failure planes were measured at 30◦. The width of the fractured area varied from the width of the CFRP strip (½") to about 1-½". The length of the fractured are was 75% of the total depth of the beam.

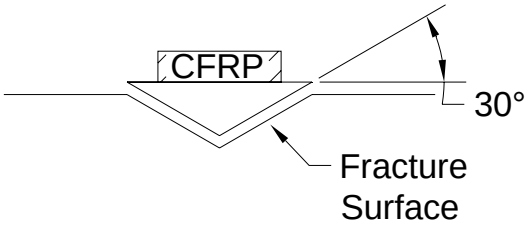

Fig. 21 – Geometry of failure under CFRP strip (top view)

An expression of the following form, to model this mode of failure, is proposed:

$$V_{cf} = \frac{1.5 h w_{cf} \left(6\sqrt{f_c'}\right)}{\cos 30} \tag{4}$$

in which h is the overall beam depth, w_{cf} is the width of the CFRP strap, and f_c' is the unconfined concrete strength.

The capacity equation is thus modified to

$$V_u \le \phi V_n = \phi\left(V_c + V_s + V_{cf}\right) \tag{5}$$

Table 3 compares the measured results for the CFRP-reinforced beams with Eqn. 5.

Beam	Loading	$V_{measured}$ (kips)	$V_{max,\ predicted}$ (Eqn. 5) (kips)
3	Static	30.82	29.04
4	10^5 cycles	30.82	28.45
6	10^6 cycles	28.81	28.45

There is the possibility that Eqn. 5 is non-conservative in the 10^6 cycle range and above, but more testing in needed to determine this.

It is clear that, while these beams failed as a result of concrete rupture under that CFRP strap, failure of the strap itself must also be considered. Thus, a formal version of Eqn. 4 would take the form:

$$V_{cf} = \min\left\{\begin{array}{c} \dfrac{1.5hw_{cf}\left(6\sqrt{f_c'}\right)}{\cos 30} \\ \\ \dfrac{f_{cf}A_{cf}d}{s} \end{array}\right\} \qquad (6)$$

in which f_{cf} is the ultimate strength of the carbon fiber, A_{cf} is the total area of carbon fiber in one strap, and s is the strap spacing.

CONCLUSIONS

While this series of tests was of course limited, some conclusions and inferences may be drawn. These may have ramifications for the design and analysis of retrofits to understrength beams, and to unretrofitted beams subjected to high numbers of load cycles.

The main conclusion arising from this series of tests is that cycling of a cracked beam externally-reinforced for shear with CFRP will place a large proportion of the shear load on the CFRP. This means that either the CFRP, or more likely the concrete under the bonded reinforcement, will become the critical element in the system.

The ramification of this is that CFRP reinforcement of a beam which has been found to be cracked in service, and which is subject to cyclic loading, should be designed for adequate strength assuming that the CFRP will carry nearly the full applied shear load. Both the strength of the CFRP itself, and the tensile strength of the concrete under the bonded strap must be taken into consideration. In the latter case the width of the strap will most likely be the critical design parameter.

Also, the stiffness of shear-critical CFRP-reinforced beams will decrease after cracking. This can be important in structures that experience extreme-event loading (seismic or blast), in that a reduction of stiffness in an individual element will ‘throw’ shear to a stiffer element. In these cases such beams must be given an appropriate constitutive representation. This conclusion may also apply to non-retrofitted beams subjected to high numbers of load cycles.

Finally, Eqn. 5 is seen to predict the shear strength of the CFRP-reinforced beams with good agreement to observed results.